Possibility of baryon number violation at hot spots in relativistic heavy-ion collisions

Rajarshi Ray *, Soma Sanyal †, and Ajit M. Srivastava ‡
Institute of Physics, Sachivalaya Marg, Bhubaneswar 751005, India

Abstract

It is possible that under certain situations, in a relativistic heavy-ion collision, partons may expand out forming a shell like structure. We analyze the process of hadronization in such a picture for the case when the quark-hadron transition is of first order, and argue that the inside region of such a shell must correspond to supercooled (to $T = 0$) deconfined vacuum. Hadrons from that region escape out, leaving a bubble of pure deconfined vacuum with large vacuum energy. This bubble undergoes relativistic collapse, with highly Lorentz contracted bubble walls, concentrating entire energy into extremely small regions. Eventually bubble walls collide, with the energy being released in the form of particle production. Thermalization of this system can lead to temperatures of the order of several GeV for RHIC energies, and may even exceed the electroweak transition temperature ($\sim$ 100 GeV) for LHC. We discuss implications of such hot spots, most importantly about the possibility of observing sphaleron transitions and resulting baryon number violation in heavy-ion collisions at LHC. Even for RHIC, such high temperatures will have clear signals, in terms of very large P_T partons, dileptons, and enhanced production of heavy quarks. Due to concentration of large energy at these hot spots, possibility of Higgs and top quark production may also arise.

PACS numbers: 25.75.-q, 12.38.Mh, 98.80.Cq

Typeset using REVTEX

*e-mail: rajarshi@iopb.res.in

†e-mail: sanyal@iopb.res.in

‡e-mail: ajit@iopb.res.in

I. INTRODUCTION

There are strong reasons to believe that in ultra-relativistic collisions of heavy nuclei, a hot dense region of quark-gluon plasma (QGP) may get created. There is a wealth of data which strongly suggests that already at CERN SPS this transient QGP state may have been achieved [1]. With new data already coming out from RHIC at BNL [2], it may be only a matter of time that conclusive evidence of QGP detection would be obtained. Certainly, one expects that at LHC (in next few years) QGP will be produced routinely. There is no question that detection of this new phase of matter will be of utmost importance, not just for testing predictions of QCD, but also in providing us glimpses of how our universe may have looked like at few microseconds of age. It seems to be an appropriate stage that one starts looking beyond the detection of the QGP phase. Many interesting possibilities have been discussed in literature about physical processes which may become observable once QGP is produced in laboratory. For example, one will have the opportunity of studying phase transitions in a relativistic field theory system under controlled laboratory situations. The richness of QCD phase diagram may become available for probing with quark-hadron transitions occurring in these experiments [3].

In this paper we propose a novel possibility of achieving extremely hot, tiny regions in these relativistic heavy-ion collisions, with temperatures far above the initial temperature of the QGP system. We assume that the confinement-deconfinement phase transition is of first order, and show that such hot spots will arise if the parton system (formed in the collision) expands out in a shell like structure, leaving behind the supercooled deconfined phase with large vacuum energy density. Eventually, as the partons hadronize and escape out, the interface, separating this false vacuum bubble from the confined phase outside, undergoes relativistic collapse. Due to absence of any plasma inside, the motion of this interface becomes ultra-relativistic, with highly Lorentz contracted interface thickness. Entire energy of the false vacuum bubble gets converted to the kinetic energy of the wall. Eventually different portions of bubble wall collide, converting the entire energy into particles. These particles may thermalize and lead to an extremely hot, very tiny region. We find that at RHIC energies, the temperatures at these hot spots can be several GeV, and may even reach as high as about 30 GeV (for certain choice of parameters). This will have important signals such as increased production of heavy quarks, anomalously large values of P_T of some hadrons (those coming from the hot spot) etc. Also, the net energy of the hot spot may be very large in some cases ($\sim$ 1 TeV), hence the possibility of Higgs and top quark production may also arise (depending on the decay products of the bubble wall). At LHC energies, we show that the temperature in these *hot spots* may even exceed the electroweak phase transition temperature of about 100 GeV, with the size of the region being of the order of $(100\ \mathrm{GeV})^{-1}$. This raises the possibility that sphaleron transitions may occur in these regions (depending on the size of such a region), which will lead to baryon number non-conservation. It is needless to say that any possibility of detection of electroweak baryon number violation in laboratory experiments deserves serious attention, especially with its implications for the theories of baryogenesis in the early universe.

We mention here that the possibility of baryon number violation in collider experiments has been discussed earlier, see, ref. [4] and references therein. However, the discussion in these works was about possibility of baryon number violation at high energies, and not at

high temperatures. It is fair to say that at this stage it is not clear whether it is possible to get baryon number violating interactions at high energies. However, baryon number violation at high temperatures (with temperatures near or above the electroweak scale) is on rather strong foundations [5–7]. Our model is based on this high temperature baryon number violation.

The paper is organized as follows. In section II, the basic physical picture of the model is discussed where it is argued how a shell enclosing deconfined vacuum may form in ultra-relativistic heavy-ion collisions. Section III discusses the properties of the shell, the surface energy, volume energy etc. Section IV discusses the evolution of this shell and its final ultra-relativistic collapse leading to high concentration of energy in a tiny region. Section V presents results for various ranges of parameters, for LHC and RHIC energies. Discussion of results and conclusion is presented in section VI.

II. PHYSICAL PICTURE OF THE MODEL

The main aspect of our model is based on the observation (discussed in the literature [8]) that under certain situations, the expanding parton system may form a shell like structure. This type of picture emerges under a variety of conditions. For example, in a hydrodynamical expansion, the rarefaction wave reaching center gives rise to a shell like structure [8]. (We mention, that shell like structure with a *maximum* of density at center has also been discussed in the literature [9].) It has been shown that shell structure will arise generically in an expanding parton system when partons are ultra-relativistic and particle collisions are not dominant [8]. This happens for the simple reason that with all partons having velocity $\simeq c$, the partons pile up in a shell of radius $\simeq c \times t$, with the thickness of the shell being of the order of the size of the initial region. Indeed, the original so called *baked Alaska* model for the disoriented chiral condensates, proposed by Bjorken et al. [10] utilizes a shell like picture for the expanding parton systems (see also, ref. [11] where a similar picture has been discussed). Our model is based on this generic shell structure of the parton system.

However, there is one important difference between our model and other discussions in the literature where a shell like structure of partons has been discussed. In refs. [10,11], the discussion was in the context of a second order chiral phase transition where the larger potential energy of the inside region slowly decreases as the chiral field relaxes towards the true vacuum. In contrast, our model is based on a first order confinement-deconfinement phase transition, where the vacuum energy of the inside region can only decrease by collapse of the interface (or, via nucleation of true vacuum bubbles in this region, which we argue to be very suppressed). Though we have presented the discussion in terms of a first order deconfinement-confinement transition, our entire discussion will also be valid for a first order chiral phase transition. Basic energy scales of these two transitions being roughly of same order, even quantitative aspects of the discussion will not change much. In discussions of [8] it is argued that the hadronization in the shell will proceed from the inner boundary of the shell, as well as the outer boundary of the shell. This assumes that the *empty* region inside the shell will be in the confined vacuum. We argue below that there is no reason to expect that. Rather, one expects that the shell of partons will enclose a region of deconfined vacuum.

Let us start with the initial stage of central collision of two nuclei. For very early stages after the collision, the region between the two receding nuclei will be populated by a dense system of partons, with a temperature which is expected to be well above the critical temperature T_c of deconfinement-confinement phase transition (say, at RHIC and LHC). (We will consistently refer to the phase transition as the deconfinement-confinement (D-C) phase transition rather than using the conventional terminology of quark-hadron transition. This is because we will utilize the difference between the vacua of the two phases of QCD, irrespective of the fact whether these vacua are populated by quark-gluon, or hadron degrees of freedom.) Subsequently, plasma will expand longitudinally for early times (for $\tau < R_A$, where τ is the proper time and R_A is the radius of the nucleus), and will undergo three-dimensional expansion for larger times. For heavy nuclei with large A, and for center of mass energies at RHIC and LHC, it is expected that the plasma will undergo deconfinement-confinement phase transition during this three dimensional expansion stage, and later the expanding hadronic system will freezeout. In various models of freezeout, it is argued that the freezeout happens soon after the D-C phase transition and that this stage is achieved at proper time hypersurface which is close to the hypersurface when three-dimensional expansion commences [12] (see, also ref. [13]).

The expected value of central energy density ϵ_i at the initial stage (hence the initial temperature T_i), increases with A and with $\sqrt{s}$. An estimate of the dependence of ϵ_i on A and $\sqrt{s}$ can be obtained from the scaling relations proposed in ref. [14] (see also, ref. [15]),

$$\epsilon_i = 0.103 A^{0.504} (\sqrt{s})^{0.786} \text{ GeVfm}^{-3}, \tag{1}$$

where $\sqrt{s}$ is in GeV. These scaling exponents reproduce the expected values of initial energy density for SPS, RHIC and LHC. Thus, for LHC, with $A = 208$ and $\sqrt{s} = 5.5$ TeV (we will use $\sqrt{s}$ to refer to $\sqrt{s}$ per nucleon), we find $\epsilon_i \simeq 1.3$ TeV/fm^3 which is within the range of other estimates [16].

We note that dependence on A is somewhat weaker than the dependence on $\sqrt{s}$. Thus, if one decreases value of A and increases $\sqrt{s}$ suitably, one can still get large ϵ_i (suitable for having a QGP state initially at temperatures well above T_c). However, with lower value of A, R_A will be smaller ($R_A \simeq 1.1 A^{1/3}$), implying that the three-dimensional expansion will commence at earlier values of proper time. This will have two effects. Temperature will decrease faster ($T \sim \tau^{-1}$ for three-dimensional expansion while $T \sim \tau^{-1/3}$ for longitudinal expansion [17]). More importantly, with rapidly expanding system, thermodynamic equilibrium will be maintained for a shorter duration of proper time, implying that freezeout will happen earlier. In principle, there is no reason why freezeout cannot precede the D-C phase transition. In such a situation, initial thermalized QGP system expands longitudinally for a short time, then undergoes three dimensional expansion. Due to rapid 3-dimensional expansion, the system falls out of equilibrium and keeps expanding as a parton system in non-equilibrium (still with high density of partons so that no hadronization takes place yet). Eventually the parton system will be dilute enough to enter into the non-perturbative regime, and will undergo hadronization. This process of hadronization will be in a non-equilibrium state, where a parton system out of equilibrium converts to a hadron system (again, out of equilibrium). Possibility of freezeout preceding hadronization has also been discussed previously in ref. [18]. A quantitative discussion of the limiting values of $\sqrt{s}$, and that of A below

which freezeout may precede hadronization, can only be given using elaborate numerical computations (such as those in ref. [12]).

In such a picture of expansion of parton system, it is possible to have the central region (in the shell) depleted of partons while the partons get accumulated in the shell. Thus, central region does not *cool* to become zero temperature, zero density QCD matter, as would happen if the system was always in thermal equilibrium (and that would then require that the interior of the shell be in the confined vacuum, as assumed in [8]). On the other hand, in the above picture, the interior of the shell is depleted of partons because of rapid expansion of the parton system. As thermal equilibrium is not maintained, parton collision rate lags behind the expansion rate. As mentioned above, in such a situation the analysis of refs. [8] suggests that partons, due to their relativistic velocities, pile up in a shell of radius $R \simeq c \times t$ where t is the time in the center of mass frame of the collision. The thickness of the shell Δr will be expected to be of the order of the size of the region when thermal equilibrium is first broken such that parton system undergoes almost free expansion after that.

We mention here that it is conceivable that the initial parton system never thermalizes (for example for very small A), but nevertheless, deconfinement phase is achieved. This possibility originates from the discussions of non-thermal symmetry restoration in the context of inflation in the early universe [19]. In these works it is shown that rapid particle production due to parametric resonance can lead to modification of the effective potential, even without any notion of thermal equilibrium. Under certain situations the symmetry restoration can be achieved even when thermal symmetry restoration is not expected. The early stages in nucleus-nucleus collisions resemble the stage of parametric resonance at least in the sense of rapid particle production. It is then possible that in this case also deconfinement phase is achieved with parton system always remaining out of equilibrium. (We will discuss this non-thermal symmetry restoration in the context of heavy-ion collisions in a future work.) This system will then undergo expansion forming a shell structure [8] before hadronizing eventually.

Thus, we assume that the expanding parton system forms a shell, with the interior of the shell being in the deconfined vacuum. At the outer boundary of the shell there must be an interface separating the deconfining vacuum in the interior from the confining vacuum in the outer region [20]. (We are assuming the D-C transition to be of first order, with a barrier separating the metastable deconfined vacuum from the true confining vacuum, even at temperatures approaching zero. We will discuss this issue in detail below. Partons will be piled up inside the shell, within a thickness Δr of the interface. The center of the shell interior thus represents a supercooled (to $T = 0$) region trapped in the metastable deconfining vacuum.

It is somewhat uncommon to talk about zero temperature deconfining phase of QCD. Normally one associates deconfinement phase with the quark-gluon plasma at temperatures above T_c. However, it is important to distinguish the vacuum of a theory from the particle excitations about that vacuum. Confining phase and the deconfining phase of QCD correspond to the two different vacua of the theory, with the deconfining vacuum being metastable at zero temperature. The two vacua may be characterized by an order parameter, such as the expectation value of the Polyakov line [21]. That means that certain type of gauge field background leads to one vacuum, while a different gauge field background gives the differ-

ent vacuum. These two vacua are thus defined irrespective of the presence or absence of quarks and gluons as particle degrees of freedom (except as test particles in order to define confinement). It then makes sense to talk about deconfining vacuum without any quark or gluon being present, though this vacuum will be metastable.

The type of picture we are taking in our model, with the shell interior depleted of quarks and gluons but still trapped in the metastable deconfining vacuum, is very similar to what happens in the inflationary theories of the universe [22]. For example, in the old inflation, the scalar field ϕ gets trapped in the false vacuum and supercools as the universe undergoes exponential expansion due to the non-zero potential energy of ϕ. Initially the universe is filled with scalar particles (as well as other particles) in thermal equilibrium corresponding to a temperature above the transition temperature. However, due to exponential expansion, initially the system cools maintaining equilibrium, but then falls out of equilibrium with all particles undergoing depletion due to exponential expansion of the universe. Eventually the particles are completely diluted away, while the universe still remains in the metastable vacuum. This is precisely the same picture as we are using in our model. The only thing required for such a picture is that QCD admit a metastable vacuum even at zero temperature. The exponential expansion of the universe is replaced by rapid outward expansion of partons in our case. Possibility of supercooling and a brief inflationary phase at quark-hadron transition in the universe has also been discussed in the literature [23].

III. PHYSICAL PROPERTIES OF THE SHELL

It is perfectly sensible to believe that QCD admits a metastable vacuum even at zero temperature. The entire physics of Bag model is within this type of framework. Inside of the bag is in the deconfining vacuum which is metastable with higher potential energy (the bag constant). The region outside the bag is in the confining vacuum with zero potential energy, with a wall separating the two regions. This is entirely consistent with the picture of a first order deconfinement-confinement phase transition at finite temperature where one usually writes down a finite temperature effective potential as a function of an appropriate order parameter. The expectation value of the Polyakov line $< L >$ has been used to describe the physics of this phase transition at finite temperature [21], where $< L >$ is given by,

$$< L >= \frac{1}{N_c} < trPe^{i\int_0^\beta A_0 d\tau} >, \tag{2}$$

where N_c is the number of colors, $\beta = 1/T$, P denotes path ordering, and A_0 is the time component of the vector potential. $< L >$ vanishes in the confining phase, while it is non-zero in the deconfining phase, breaking the Z(3) symmetry spontaneously [21].

On the other hand, at $T = 0$, the physics of bag model can be captured by postulating a color dielectric field χ with the following form of the effective potential for χ [24,25],

$$V(\chi) = \frac{m_{gb}^2}{2}\chi^2[1 - 2(1 - \frac{2}{\alpha})\frac{\chi}{\sigma_v} + (1 - \frac{3}{\alpha})\frac{\chi^2}{\sigma_v^2}]. \tag{3}$$

with corresponding Lagrangian density being $L = \frac{1}{2}(\partial_\mu\chi)^2 - V(\chi)$. Here, $\sigma_v = \sqrt{2\alpha B/m_{gb}^2}$, m_{gb} is the glueball mass, B is the bag constant, and we take $\alpha = 24$, $B^{1/4} = 122.3$ MeV,

and $m_{gb} = 978.6$ MeV. These are the parameter values used in ref. [24], and we use these as a sample. The relevance of these parameters for us is in determining the values of surface tension σ and false vacuum energy density ρ of the deconfining bubble. We will present results for a wide range of σ and ρ.

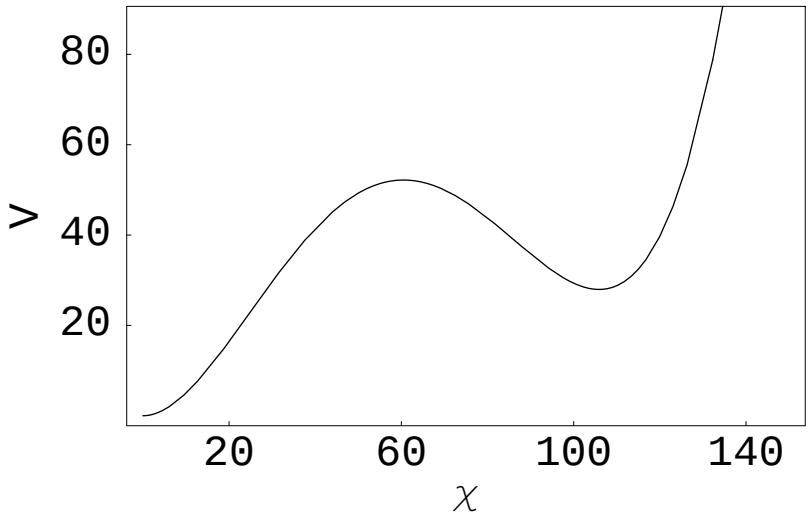

FIG. 1.
Plot of $V(\chi)$ (in MeV/fm^3) vs. χ (in MeV), as given in Eq.(3). The absolute minimum at $\chi = 0$ corresponds to the confining true vacuum while the local minimum at $\chi \neq 0$ corresponds to the metastable deconfining vacuum.

The plot of $V(\chi)$ is shown in Fig.1. Thus, $\chi = 0$ in the confining region outside the bag, while it has a non-zero value in the deconfining region inside the bag. χ thus has the same physical behavior as $< L >$, the expectation value of the Polyakov line L. It would seem rather superfluous to have two entirely different characterizations of same physical phenomenon, i.e. two different phases of the same system, separated by an interface. One would like to think of the color dielectric field χ as capturing the physics of $< L >$. With this identification, one has a single, unifying picture where the effective potential for a strongly interacting system is always of the form given in Eq.(3), with χ being interpreted as either the color dielectric field of the bag model, or the expectation value of the Polyakov line L. At finite temperature, the coefficients in $V(\chi)$ will become temperature dependent which will change the values of surface tension of the interface, latent heat etc. compared to the values

obtained from the parameter values given above. The important thing is that the barrier between the deconfining vacuum and the confining vacuum must survive even at $T = 0$ if the physics of the bag model has to be preserved. We mention that the forms of effective potential such as the one used in ref. [26] do not capture this physics of deconfinement-confinement phase transition. For example, in ref. [26], an effective potential has been used with a $T\phi^3$ term (with ϕ being the order parameter for D-C phase transition) to model the first order nature of the transition. Thus in this model, barrier between the deconfining vacuum and the confining vacuum disappears below certain temperature, which is not in the spirit of the physics of bag model.

The final picture of our model can now be presented. We start with the initial time τ_i, with dense partons filling the collision region. This parton region will correspond to the region between the two nuclei, receding after overlap, with transverse radius of the region being equal to R_A, the nuclear radius. Much of the collision energy will be carried by partons in the fragmentation region. We are interested in the total energy available to the expanding parton system in the central region, which will eventually lead to the formation of the false vacuum bubble. For this, we take the total energy E_{tot} to be,

$$E_{tot} = \epsilon_i \pi R_A^2 \Delta z_i, \tag{4}$$

where ϵ_i is the initial energy density expected in the collision (as given in Eq.(1)). $R_A \simeq 1.1A^{1/3}$ fm, and Δz_i is the initial thickness of the central region. For central region near $z = 0$, Δz_i corresponding to a rapidity interval ΔY at the initial time τ_i can be taken as $\Delta z_i = \tau_i \Delta Y$ (see, ref. [15]). Estimates for τ_i, initial QGP formation time, vary from $\tau \sim 0.1$ fm (for LHC) to $\tau \sim 0.2$ fm for RHIC. In view of various uncertainties [14–16] in the estimates of ϵ_i, and τ_i, (as well as in determining the relation between the plasma formation time τ_i and the initial longitudinal extent of the plasma), we will present results for a range of values of Δz_i. We will take $\Delta z_i = 0.15$ fm for LHC, and equal to 0.22 fm for RHIC, and an optimistic value $\Delta z_i = 1$ fm for both LHC and RHIC which will correspond to a large value of E_{tot}. It is important to mention that our results only depend on the value of E_{tot}. Thus, large value of E_{tot} may arise from uncertainties in ϵ_i, or Δz_i. For Pb-Pb collision at LHC with $\sqrt{s} = 5.5$ TeV, expected initial energy density in the central region is about 1.3 TeV/fm^3. This gives $E_{tot} \simeq 25$, and 175 TeV corresponding to $\Delta z_i = 0.15$, and 1 fm respectively. For Au-Au collision at RHIC with $\sqrt{s} = 130$ GeV, the energy is much smaller and we find $E_{tot} \simeq 2$, and 9 TeV for $\Delta z_i = 0.22$, and 1 fm respectively.

This parton system then expands and cools (for non-equilibrium expansion, we say that the energy density of parton system decreases as temperature may not be defined). Important thing is that at the initial time τ_i, the parton system must be in the deconfining phase (either due to temperature $> T_c$, or due to non-thermal transition with extremely high energy density of partons). The region outside the initial parton system being in the confining phase, there must be an interface separating the two regions. Fig.2a shows such a situation.

Initial expansion will be longitudinal for proper times $\tau < R_A$, and will become three-dimensional expansion for larger times. It is expected that energy density (or the temperature) still remains sufficiently high so that by the time expansion becomes three-dimensional, the parton system still remains in the deconfining phase. Fig. 2b denotes such a stage of

the central parton system at $\tau \simeq R_A$. (We mention here that it is not crucial for our model whether the fragmentation region is inside this region shown in Fig.2b, or falls outside it.) For subsequent expansion, we assume (as explained in detail above) that a shell structure starts developing. For times much larger than R_A, one expects an almost complete depletion of partons in the central region [8], with all partons piled up near the shell boundary. Fig. 2c denotes this intermediate stage. (We can take the proper time τ as measured in a frame at rest at some average point in the middle of the shell. Velocity there will not be very close to c, so τ will not be much different from the time t in the center of mass frame. In any case, the 3-dimensional expansion is not expected to be ultra-relativistic, so at this stage, one can use τ and lab time t interchangeably. We also neglect any Lorentz contraction in the thickness of the parton shell.) The stage shown in Fig.2c is the non-trivial part of our model. Here, the entire region inside the sphere of radius $\simeq ct$ is taken to be in the deconfining vacuum. There is then the interface at the boundary. The partons accumulate near the inner boundary of the shell. The thickness of this region containing the partons will be expected to be of order of about $2 \times R_A$ as that is the total extent of the region at the time at which three dimensional expansion began.

The region with $r < ct - 2R_A$ has no partons, but is still in the deconfining vacuum. This somewhat unconventional picture can be further justified as follows. Starting from a stage as shown in Fig.2b, where the entire interior region was in the deconfining vacuum, one reaches the stage shown in Fig.2c by parton expansion. The inner region (devoid of partons) can turn into the confining vacuum only if there is nucleation of bubbles of confining vacuum in that region, which upon coalescing will convert the inner region into the confining vacuum. This could happen if the inner region cooled to $T = 0$ (with zero parton density, assuming zero baryon number in the central region) maintaining thermal equilibrium. However, thermal nucleation of bubbles could not happen since we are assuming that freezeout occurred before the hadronization transition (or, due to large time scales of bubble nucleation [27]). If the system did not go through finite temperature bubble nucleation when temperature decreased below T_c, then inside region can still be in the confining vacuum if quantum nucleation of confining vacuum bubbles (at $T = 0$) could happen. As we will discuss below, the action S_0 of such a bubble is about 100 in natural units. The probability of nucleation of such a bubble is proportional to e^{-S_0}, and hence is completely negligible for the relevant time scales, allowing for reasonable dimensional estimates for the pre-factor for the nucleation probability. (As in our model a significant barrier separating the two vacua remains even at $T = 0$, there is no possibility of the phase transition occurring via spinodal decomposition.) Thus, we conclude that the inner region of the shell must correspond to $T = 0$ supercooled deconfining vacuum.

Eventually, as parton shell keeps expanding, its energy density falls below a critical value so that hadronization must take place. Partons will then form hadrons and will leave the spherical region bounded by the interface. This is the stage when the interface will stop moving outward, and will start shrinking. As the interface passes through the parton system, it converts partons into hadrons, as shown in Fig.2d. The motion of the interface will be dissipative at this stage due to its interaction with partons. Typical velocity of the interface, therefore, will be less than the speed of sound [28,26,27]. However, as all (or most) of the partons hadronize, the interface will continue to move inward (due to negative pressure of the metastable vacuum). Now there are no partons to impede the motion of the interface.

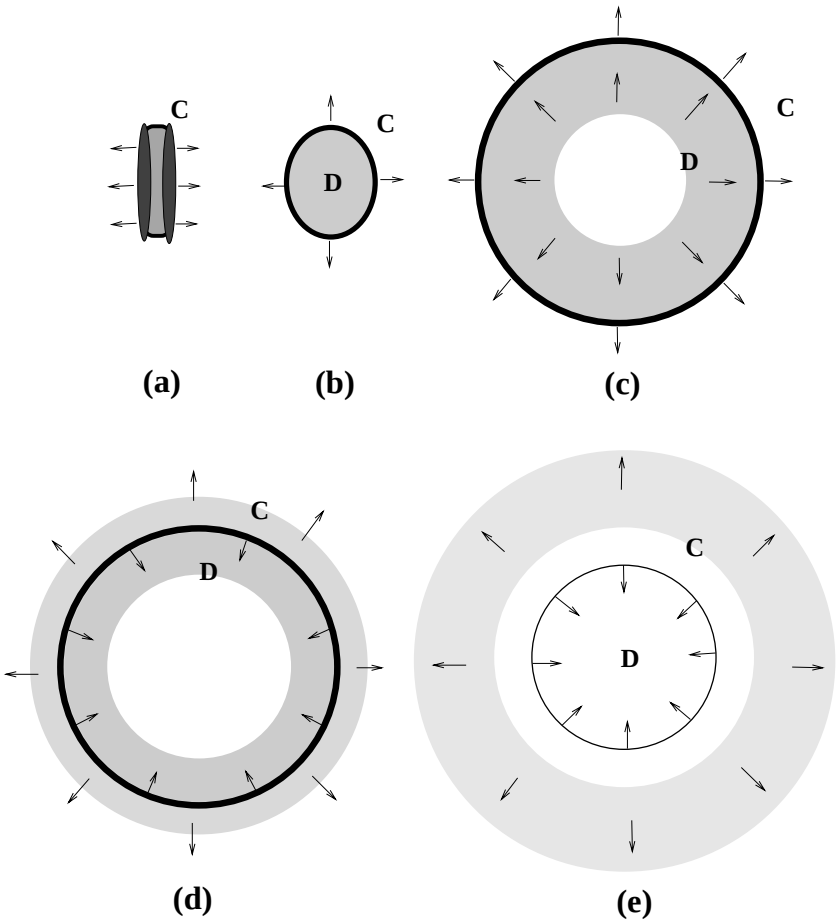

FIG. 2.
(a) The initial stage showing beginning of longitudinal expansion of the parton system between the two nuclei receding after overlap. (b) Beginning of transverse expansion. C and D denote regions with confining vacuum and deconfining vacuum, respectively. Thick solid line at the boundary denotes the interface separating the two vacua. (c) Development of shell structure with depletion of partons in the center due to expansion. (d) Stage of hadronization of the parton shell as the interface shrinks through the shell. (e) Relativistic collapse of the interface. Interface is shown to be thinner due to Lorentz contraction.

What one is left with is a spherical bubble of pure false vacuum. To obtain the profile of the wall of this *false vacuum* bubble, we first obtain the profile of the *true vacuum* bubble as follows. Given $V(\chi)$ in Eq.(3), one can obtain the instanton solution for the tunneling through the barrier from $\chi \neq 0$ metastable vacuum to the $\chi = 0$ true vacuum. This is given by the solution of the following equation [29],

$$\frac{d^2\chi}{dr^2} + \frac{\kappa}{r}\frac{d\chi}{dr} - V'(\chi) = 0, \tag{5}$$

where $V(\chi)$ is the effective potential in Eq.(3) and r is the radial coordinate in the Euclidean space. In the Minkowski space initial profile for this true vacuum bubble is obtained by

putting $t = 0$ in the solution of the above equation. Parameter $\kappa = 3$ for quantum nucleation of bubble (at $T = 0$), while $\kappa = 2$ for thermal nucleation of bubble at finite temperature. Initially the parton region had large temperature, so the profile of the interface at that stage would be given by the finite temperature bubble (i.e. $\kappa = 2$). This will be true up to the stage shown in Fig.2b. After freezeout, or once the partons leave the shell in the form of hadrons as in Fig.2e, the profile of the interface will be given by $T = 0$ bubble, that is $\kappa = 3$ case. We have solved Eq.(5) using a fourth order Runge Kutta algorithm for the effective potential as given in Eq.(3). The numerical technique is the same as used earlier for standard false vacuum decay [30] with the obvious difference that now the false vacuum occurs at non-zero value of χ while the true vacuum occurs at $\chi = 0$. Thus the search for the bounce solution has to be done differently in the present case. In Fig.3a we have shown the solution of the $T = 0$ quantum bubble of true vacuum. The radius of this bubble is about 5 fm. (The finite temperature bubble has a smaller radius $\simeq 3.8$ fm.) We have calculated the action for the true vacuum bubble shown in Fig.3a and we find it to be about 100 in natural units. As mentioned above, this large value of the action suppresses the nucleation of true vacuum bubbles in the the central deconfined (T = 0) region, so that this region converts to the confining vacuum only via collapse of the spherical interface shown in Fig.2e.

Fig.3a shows the bubble of confining vacuum embedded in the deconfining vacuum (as obtained by the instanton solution of Eq.(5)). However, the experimental situation we have discussed above is exactly the reverse. As shown in Fig.2e, we have a large bubble of deconfining vacuum which is embedded in the confining vacuum. Such a bubble cannot be obtained as a classical solution of Eq.(5). The situation shown in Fig.2 arises because of changing temperature, and is similar to the false vacuum bubble formation due to coalescence of true vacuum bubbles as discussed in the context of quark-hadron transition in the early universe [31]. Main difference between our case and the case discussed in ref. [31] (see, also ref. [27]) is that there the motion of bubble wall remains dissipative due to presence of QGP in the interior of the bubble. In contrast, in our case, the special geometry of collision gives the shell like structure which leads to a pure false vacuum bubble with no QGP inside. The motion of the interface, therefore, will not be dissipative. Fig.3b shows this false vacuum bubble which is simply obtained by inverting the profile of the bubble as given in Fig.3a. This is a somewhat approximate way of generating the appropriate bubble profile. However, our interest is only in the values of surface tension σ of the interface and the false vacuum energy density ρ. (Note that ρ is the same as the bag constant B. We use a different notation for it due to the method by which we calculate it by generating the confining vacuum bubble and then inverting it.) We will present results for a range of values of these parameters, with the profile given in Fig.3b corresponding to one set of these values. Note that the radius of this deconfining vacuum bubble (Fig.3b) is not obtained from equation of motion. In contrast, radius of the confining vacuum bubble of Fig.3a was fixed by the solution of Eq.(5). Inverted profile in Fig.3b is generated only to estimate the values of σ and ρ corresponding to parameter values in Eq.(2). Its radius will be determined by the physics of the problem, such as total energy of collision, as we discuss below. In the same way, the radius of the false vacuum bubble in ref. [31] is determined by separation between the nucleation sites of the hadronic bubbles, and the manner in which they coalesce.

To obtain values of surface tension σ and the false vacuum energy density ρ of the deconfining vacuum bubble, we obtain total energy E of the false vacuum bubble by numerically integrating $\frac{1}{2}(\bigtriangledown\chi)^2 + V(\chi)$ for the bubble profile in Fig.3b. Bubble energies are obtained in

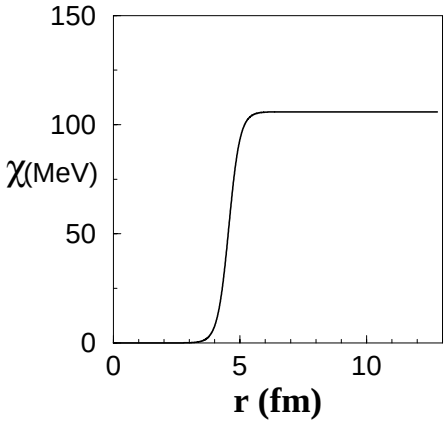

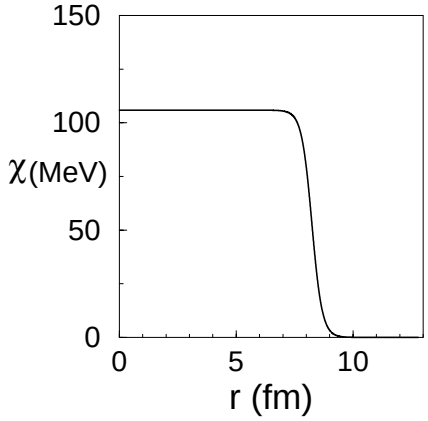

FIG. 3.
Left figure shows the true vacuum quantum bubble obtained as the solution of Eq.(5). Right figure shows the false vacuum bubble obtained by inverting the profile of the true vacuum bubble. χ is in MeV and r is in fm.

this manner for two different values of bubble radius. σ and ρ are then determined by using the following equation for the two values of bubble energy and radius,

$$E = 4\pi r^2 \sigma + \frac{4\pi}{3} r^3 \rho. \tag{6}$$

The values of σ and ρ obtained by using this equation for two values of bubble radius are

tested for other bubble radii and it is found that bubble energies are accurately reproduced. For the parameter set of Eq.(3) [24], we find $\sigma = 64.8\text{MeV/fm}^3$ and $\rho = 27.8\text{MeV/fm}^3 (\simeq (122\text{MeV})^4)$. Note that this value of ρ is the same as the bag constant B of Eq.(3) as it should be. This gives us confidence that this procedure of inverting profile of confining vacuum bubble to get the profile of the deconfining vacuum bubble is reasonably accurate. For comparison, we repeated this procedure for the finite temperature bubble, i.e. solution of Eq.(5) with $\kappa = 2$, (pretending that the effective potential in Eq.(3) corresponds to the finite temperature case). As we mentioned, resulting bubble radius of the confining vacuum bubble (similar to the $T = 0$ bubble in Fig.3a) is about 3.8 fm. We find that the inverted bubble (deconfining vacuum bubble, as in Fig.3b) has $\sigma = 64.4$ MeV/fm^2 and $\rho = 27.8$ MeV/fm^3. These values are essentially the same as in the case of $T = 0$ bubble. Since the only thing we need from the above calculations is the values of these parameters, it is immaterial whether we think of the interface as corresponding to the finite temperature bubble or to $T = 0$ bubble.

IV. EXPANSION AND SUBSEQUENT ULTRA-RELATIVISTIC COLLAPSE OF THE SHELL

We need to make one further specification about the expansion of the parton system. If the expansion is adiabatic, then total entropy will be conserved. In that situation, total energy will decrease due to the work done by the pressure of the plasma. This description is appropriate when expansion happens maintaining equilibrium, as in the hydrodynamical models of parton expansion. In the situation of free expansion, or if there are dissipative effects present, then expansion could be energy conserving [32]. For adiabatic expansion, expected temperatures of the hot spot are smaller. We have argued above that shell picture is more reasonable in the case when parton system freezes out early. Thus energy conserving expansion may be more appropriate for our model. We consider this case first. We will also briefly discuss results for the adiabatic expansion. (Note that the only thing relevant to us about the parton expansion is the development of a shell structure with central region devoid of partons, but still in the deconfined vacuum. We have argued that this seems natural when partons freezeout early. However, all of our arguments are valid if this picture can be justified even by taking partons to be in equilibrium, through the stages in Fig.2a-2d.) Assuming the energy to be conserved, the energy density of the partons in the shell, $\epsilon(r)$, at any stage shown in Fig.2c, is determined by,

$$4\pi r^2\sigma + \frac{4\pi}{3}(r^3 - (r - \Delta r)^3)\epsilon(r) + \frac{4\pi}{3}r^3\rho = E_{tot}, \tag{7}$$

where E_{tot} is given in Eq.(4). Here $\epsilon(r)$ denotes the parton energy density in the shell of thickness $\Delta r \simeq 2R_A$. The shell will expand to a largest size r_{max} at which stage parton system will hadronize. We determine r_{max} by taking $\epsilon(r) = \epsilon_c$, the critical value of energy density of partons below which hadronization is expected to take place. We take $\epsilon_c \simeq \frac{\pi^2 37}{30} T_c^4$, where T_c is the critical temperature for the quark-hadron transition. ϵ_c is not to be taken necessarily as the energy density of plasma in equilibrium (with temperature $= T_c$), as we have argued that the partons may be in a non-equilibrium state. We take ϵ_c as giving the

scale below which partons should convert to hadrons. The value of T_c is related to the bag constant (for an equilibrium transition) using Gibbs criterion of equal pressure at transition temperature, $T_c = (B/(g_q - g_h))^{1/4}$. Here, $g_q = 37\pi^2/90$ and $g_h = 3\pi^2/90$, corresponding to 2 massless quark flavors and 8 gluons in the QGP phase, and 3 pions in the hadronic phase. Again, the value of B here should be taken to be the value appropriate at $T = T_c$, which may be different than the value of B at $T = 0$. For simplicity, we ignore any temperature dependence of B and use the same value of B which equals the false vacuum energy density ρ, as also determining T_c via above relation.

r_{max} gives the largest radius of the shell, with interface being at the outer boundary (i.e. at $r = r_{max}$) initially. As this is the stage when hadrons start forming, interface starts moving inwards. Initial motion of the interface is highly dissipative [28,26], as long as it traverses the region which is filled with the partons, i.e. a thickness of $\Delta r \simeq 2R_A$. This stage is shown in Fig.2d. Once the interface has shrunk below this parton filled region, it is free to undergo unimpeded, relativistic collapse. The region bounded by this interface at a later stage (shown in Fig.2e) represents a pure false vacuum bubble with no partons inside. The initial radius of this pure false vacuum bubble, r_f will be approximately given by,

$$r_f \simeq r_{max} - R_A, \tag{8}$$

where r_{max} is determined by solving Eq.(7) with $\epsilon(r) = \epsilon_c$. In writing this expression for r_f, we have taken that when $\epsilon(r) = \epsilon_c$ is achieved during the shell expansion, the interface starts collapsing with almost speed of light, as the parton shell keeps expanding relativistically. However, due to dissipative motion of the wall through the parton system, velocity of the wall will be typically much smaller than the speed of light [28]. If one takes the wall to be almost static, as compared to the outward velocity of the shell, then one will expect r_f to be almost equal to r_{max}. Thus, the value of r_f as given above is an underestimate. Resulting total energy of the false vacuum bubble, and hence the final temperature of the hot spot will also be somewhat underestimated in using the above equation. This should hopefully compensate, to some degree, the effects of assuming all partons to be ultra-relativistic, (e.g., if the parton distribution extends beyond the assumed shell thickness of $2r_{max}$, it will reduce the value of r_f).

Total energy E_f of this pure false vacuum bubble is,

$$E_f = 4\pi r_f^2 \sigma + \frac{4\pi}{3} r_f^3 \rho. \tag{9}$$

Further evolution of this false vacuum bubble is well understood. It will undergo relativistic collapse. Due to surface tension, bubble will become more spherical as it collapses. This is important as there are various factors because of which the initial shape of the bubble wall may not be spherical. First, the collision geometry itself will not be expected to give rise to completely spherical structure. Secondly, the interface motion through the parton shell itself may not be very isotropic. However, during the free collapse of the interface, the shape should become more spherical due to surface tension. Any remaining asphericity will ultimately affect the final radius to which the bubble can collapse before the bubble walls decay via collision. For simplicity, we will assume that the interface collapses maintaining spherical symmetry. During bubble collapse, the potential energy of the false vacuum simply gets converted into the kinetic energy of the collapsing interface [29]. This is where our

model crucially differs from the collapsing QGP bubbles previously discussed in the context of quark-hadron transition [31,27]. There, interface always moves through a QGP system filling the interior of the bubble, which impedes the motion of the interface. The false vacuum energy there gets converted to the heat which raises the temperature of the plasma [31,27]. In contrast, there are no partons in the interior of the deconfining vacuum bubble in our model. The entire false vacuum energy thus converts to the kinetic energy of the interface. The collapsing interface quickly becomes ultra-relativistic, with extremely large Lorentz contraction factor, as indicated by thinner interface in Fig.2e.

At any stage during the collapse of the shell, the value of the Lorentz γ factor primarily depends on the initial radius r_f of the shell, and the value of ρ (i.e. B). To give an idea of how rapidly the bubble wall Lorentz contracts, we give values of γ at the stage when the bubble has collapsed to a radius of 1 fm. For Pb-Pb collision with $\sqrt{s} = 5.5$ TeV, and with $\Delta z_i = 1$ fm, we find that r_f varies from 20 to 90 fm as $B^{1/4}$ is reduced from 240 MeV to 120 MeV (as we will see below). Value of γ, when bubble has collapsed to a radius of 1 fm, ranges from 3×10^4 to 8×10^4. For same parameters, but with $\Delta z_i = 0.15$ fm, γ ranges from 2000 to 7000. At RHIC energy, with $\sqrt{s} = 130$ GeV for Au-Au collision (with $\Delta z_i = 1$ fm), r_f ranges from 5 fm to 20 fm as $B^{1/4}$ is reduced from 240 MeV to 120 MeV. Resulting γ factor (again, when bubble has collapsed to 1 fm radius) ranges from about 250 to 1700. For this case, by the stage when bubbles radius has decreased by another order of magnitude, i.e. to a value of 0.1 fm, γ ranges from about 3×10^4 to 2×10^5.

The thickness of the interface initially (i.e. at stages shown in Fig.2a-2d), is about 1 fm. We see that by the time bubble collapses to a radius of about 1 fm, the thickness of the interface is much smaller, about 10^{-3} fm to 10^{-5} fm. Interface thickness reduces to about 10^{-5} fm to 10^{-7} fm by the time the bubble collapses to a radius of 0.1 fm. Again, it is unconventional to talk about such large length contraction factors in the context of heavy-ion collisions. We know that due to virtual partons at small x (the so called *wee partons*), nucleus thickness does not Lorentz contract below about 1 fm even at ultra-high energies [33] (see, also, ref. [34]). However, this limiting Lorentz contraction arises due to virtual particle production in the color field of the partons. In our case, by the time the interface contracts below the partonic shell, there will be no such virtual partons inside the bubble. Thus, there is no reason to expect that the Lorentz contraction of the interface of this pure false vacuum bubble should be limited by the typical QCD scale of 1 fm. Basically, the radial profile of the interface represents the kink solution (Eq.(5)) which can be Lorentz boosted to any velocity in the absence of interactions with partons.

This extreme Lorentz contraction of the bubble wall has following important consequence. Normally, the process of the collapse of a bubble wall will stop when its radius is of the order of the thickness of the wall. (See, for example, the numerical study of collapsing domain walls in ref. [35]. Though, for ultra-relativistic collapse numerical errors can build up and one needs more sophisticated numerical techniques, see ref. [36].) Without significant Lorentz contraction, we would expect the bubble collapse to halt at the stage when bubble radius is of the order of 1 fm, as in the standard treatments of collapse of QGP bubbles in a quark-hadron transition [31]. Then bubble walls (of different bubble portions) will collide and the energy of walls will be released in the form of particle production. However, in our case the bubble wall undergoes large Lorentz contraction even when bubble radius is about 1 fm (in the center of mass frame). As compared to the wall thickness, bubble radius is about 10^3

to 10^5 times larger at this stage. Thus, there is no reason to expect that bubble collapse will halt at this stage. In fact it is easy to see (using the fact that as bubble collapses, false vacuum energy gets converted to the kinetic energy of the bubble wall) that bubble wall thickness decreases much faster (due to Lorentz contraction) compared to the bubble radius, as bubble collapse proceeds. Of course, eventually this type of *classical* evolution of bubble must stop, at least by the stage when the net size of the system has become smaller than that allowed by the uncertainty relation. The net energy E_f we start with (of the false vacuum bubble at the initial stage when free collapse of the interface commences), is much larger than a TeV. Thus, when collapsing bubble size becomes smaller than E_f^{-1} (say a TeV^{-1}), it seems reasonable that bubble collapse may halt. Entire energy E_f of the initial pure false vacuum bubble, which was subsequently converted into the kinetic energy of ultra-relativistic walls, will now get converted to particles. (It will be interesting to work out the exact conditions when bubble collapse will halt. Even if the bubble radius shrinks only to a value of say 0.1 fm, one still gets a hot spot, though with a lower temperature. It is also possible that in some situations, bubble collapse may develop strong anisotropies. In that case the bubble may break into smaller bubbles.)

It is important to realize that the above picture only requires that most, or a significant fraction, of the bubble wall energy (after bubble has collapsed to size of order 1 fm) is not dissipated away subsequently until different portions of the (Lorentz contracted) bubble wall collide with each other. This is because essentially all of the energy of the initial false vacuum bubble is already stored in the bubble walls by the time its radius shrinks to a value of order 1 fm (for initial radius much larger than 1 fm). Even with quantum fluctuations on the bubble wall background, there is no reason to expect that these fluctuations will tend to put an early stop on (or significantly dissipate the kinetic energy of) the highly relativistic bubble wall. For example, even for the case of nucleus-nucleus collision, interaction of wee partons does not stop the nuclei from overlapping at sufficiently large collision energies. Though, we again emphasize that the arguments based on limiting Lorentz contraction of a nucleus [33] cannot be applied directly to the present case of Lorentz contraction of the bubble wall.

The final conclusion is that the entire energy E_f of the false vacuum bubble will be converted to a dense system of partons, contained in an extremely tiny region which can be as small as few TeV^{-1} (or even smaller). The energy of this bubble E_f is a fraction of the total energy of the initial parton system E_{tot} as given in Eq.(4). For $A = 200$, and with Δz_i = 1 fm, this fraction ranges from 15% to 40% for $\sqrt{s} = 5.5$ TeV, and 20% to 50% for $\sqrt{s} =$ 30 TeV, as $B^{1/4}$ is decreased from 240 MeV to 120 MeV. For $\Delta z_i = 0.15$ fm, these fractions range from 5% to 20%, and 10% to 35% respectively. For RHIC, with $\sqrt{s} = 130$ GeV, and with $\Delta z_i = 1$ fm, this fraction ranges from about 3% to 15%, for the same range of $B^{1/4}$. We mention that here as well as in later sections, for LHC, we will be considering a range of values of $\sqrt{s}$, including very large values such as 30 TeV (for Pb-Pb collision). This is with the idea that any possibility of observing new physics such as the baryon number violation at such large energies, should provide strong motivation for going for such large (or even larger) values of $\sqrt{s}$.

Most of the energy of the initial parton system escapes out in the form of hadrons, and as we have seen above, only a fraction is left behind in the form of the vacuum energy inside the bubble. However, the important thing is that all this energy gets focused into a

very tiny region due to ultra-relativistic collapse of the bubble wall. The resulting energy density can be extremely high. This parton system will then expand and in that process thermalize. As we have mentioned, in some cases one can get temperatures as high as the electroweak transition temperature T_{ew}. For consistency of thermodynamic equilibrium, we must have a region of size at least of the order of T_{ew}^{-1}, where $T_{ew} \simeq 100$ GeV is the transition temperature for the electroweak symmetry restoration. (More precisely, the size of the region should be larger than the mean free paths of the relevant particle. At this preliminary stage of investigation, we will simply require that the size of the system be larger than T_{ew}^{-1}. For more careful estimates, relevant mean free paths of different particles should be taken into account. Thus, for a given size of the hot spot, some of the particles may be in equilibrium while others may freely stream out. Also, note that the evolution of the Higgs field will be governed by the time scale T_{ew}^{-1}. Thus, with $T > T_{ew}$, it should be able to relax to the symmetric vacuum for system size $\geq T_{ew}^{-1}$.) Thus, we assume that the partons resulting from eventual collision of bubble walls will thermalize by the time the size of the region is about $r_{ew} \simeq (100\text{GeV})^{-1}$. This may not be an unreasonable assumption, as this extremely dense parton system expands out from an initial size which is less than E_f^{-1}, to the size of $(100\text{ GeV})^{-1}$. With this, the resulting temperature T_f of the hot spot at this stage can be determined by the following equation,

$$\frac{g_*\pi^2}{30}T_f^4\frac{4\pi}{3}r_{ew}^3 + 4\pi r_{ew}^2\sigma' + \frac{4\pi}{3}r_{ew}^3\rho' \;=\; E_f \tag{10}$$

Here, $g_* = 37$ is the degree of freedom in the QGP phase if $T_f << T_{ew}$. However, when $T_f \sim T_{ew}$ then one must include electroweak degrees of freedom. We take $g_* = 100$, though, as we mentioned above, some of the degrees of freedom may not be in equilibrium within the size of the system of order T_{ew}^{-1} (depending on the relevant mean free paths). Smaller values of g_* will give larger values of T_f. We find that when g_* is decreased from 100 to 37, T_f (as obtained from the above equation), increases by about 30%. We will use $g_* = 100$ for calculations with LHC energies where we find the values of T_f to be typically above 50 GeV. This will result in slight underestimate of T_f via above equation. However, it will hopefully compensate for the effect of loss of those partons which stream out of the hot spot and do not thermalize. For RHIC, where T_f has much smaller values, we will use $g_* = 37$. σ' and ρ' are the values of interface tension and false vacuum energy density relevant for such high temperatures which could be above T_{ew}. Values of ρ' and σ' do not affect the value of T_f significantly when T_f is large (near or above 100 GeV). However, they become important when E_f is very small, as is the case for RHIC energies. We use QCD values for these parameters (as discussed above) for the cases when the temperature is less than 100 GeV, and use the values typical of the electroweak scale, i.e., $\sigma' \simeq T_{ew}^3$, and $\rho' \simeq T_{ew}^4$, when the temperature exceeds 100 GeV.

When T_f is exactly equal to 100 GeV, then one must allow for the changeover in the value of ρ from the value relevant to QCD to the value relevant for the electroweak symmetric vacuum (i.e., the latent heat of the electroweak phase transition). We take care of this by using the following prescription. Below, we will be giving plots of T_f as a function of $B^{1/4}$. As the value of $B^{1/4}$ is decreased, it corresponds to increasing value of E_f, and consecutively, increasing value of T_f (via Eq.(10)). For some cases, as $B^{1/4}$ is decreased, T_f increases from a value below 100 GeV, and we reach a point when T_f just equals 100 GeV (for the size of

the region equal to $(100\ \mathrm{GeV})^{-1}$). For these values of $B^{1/4}$, we use QCD values for ρ' and σ'. As $B^{1/4}$ is decreased further, E_f increases, but this increase is not enough to convert entire region of size $(100\ \mathrm{GeV})^{-1}$ into the electroweak symmetric phase (i.e., appropriate for using electroweak values of ρ' and σ'). However, a region of somewhat smaller size can always be in the electroweak symmetric phase. Equivalently, the region of size $(100\ \mathrm{GeV})^{-1}$ will be in the mixed phase. The temperature T_f will remain fixed equal to 100 GeV for these values of $B^{1/4}$. Eventually a value of $B^{1/4}$ will be reached which leads to large enough E_f which can convert the whole region of size $(100\ \mathrm{GeV})^{-1}$ into the electroweak symmetric phase. Thus, in the plots below, when T_f crosses the value 100 GeV, there will be a small range of $B^{1/4}$ for which T_f will be shown to remain constant, equal to 100 GeV.

Another important point is that, for some cases, as for RHIC, we find that the final temperature T_f as obtained from the above equation, is much smaller than 100 GeV. For such values of temperatures, it is not appropriate to consider the size of the relevant region to be given by $r_{ew} \sim (100\mathrm{GeV})^{-1}$. As we have discussed above, for the consistency of thermodynamic equilibrium, the size of the region should be at least of order T_f^{-1} (again, with a simplistic assumption that the relevant length scales are given by T^{-1}). Thus, for RHIC energy, we take the size of the region to be given by T_f^{-1} in the above equation, instead of r_{ew}. The resulting equation is 4th order in T_f which is then solved for T_f. We choose the solution of this equation which gives the largest value of T_f, as that will be the maximum temperature of the hot spot obtained with the consistency condition that the size of the hot spot is T_f^{-1}. With this, Eq.(10) determines the temperature T_f of the *hot spot*, using Eqs.(7)-(9). We emphasize again, that even if partons do not thermalize, there may still be the possibility of electroweak symmetry restoration via parametric resonance due to extremely high particle density.

V. RESULTS

We have obtained the value of T_f for a range of values of bag constant B, and for different values of A and initial energy density ϵ_i (which can be related to $\sqrt{s}$ using Eq(1)). The value of surface tension of the wall σ is taken to be 64 MeV/fm^2 (for Eqs.(7)-(9)), as determined using Eq.(6). We find that our results are rather insensitive to the value of σ. Changing σ to 1 MeV/fm^3 leads to virtually no change in T_f and r_f. (Note that this means that our quantitative results may be valid even if D-C transition is a very weak first order transition, as long as shell structure can be justified.) Increasing σ to even unreasonably large value of 300 MeV/fm^3 increases T_f by about 10 %, and decreases r_f by about 10 %. It is important not to get confused between the values of σ and ρ used for the false vacuum bubble (Eq.(6) to Eq.(9)), with the values of σ' and ρ' used in Eq.(10). σ and ρ used for the false vacuum bubble (Eq.(6)-Eq.(9)) correspond to the deconfined phase of QCD at $T = 0$. On the other hand, Eq.(10) is relevant only after the collapsing bubble walls decay into particles, and that particle system expands out forming a small hot region with very high temperatures. σ' and ρ' correspond to the surface tension and vacuum energy density relevant for this hot spot.

In Fig. 4 we have plotted T_f (in GeV) vs. $B^{1/4}$ (in MeV) for the case when Δz_i (Eq.(4)) is 1 fm. Solid, dotted, and dashed curves correspond to $A = 200$, 100, and 50 respectively. Plots have been given for $\sqrt{s} = 30, 15, 5.5$ TeV, which can be translated to the values of

$\epsilon_i \simeq 4.9, 2.8, 1.3 \text{TeV/fm}^3$, respectively (for $A = 200$). In Fig.4 we have also given plots of the radius r_f of largest pure false vacuum bubble radius for $\sqrt{s} = 5.5$ TeV. Note, the shell thickness Δr for these cases is of order $2R_A \simeq 13$ fm.

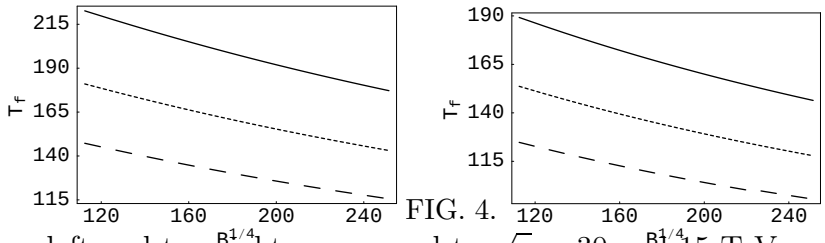

FIG. 4. Figures on top left and top right correspond to $\sqrt{s} = 30$ and 15 TeV, respectively. Bottom two figures correspond to $\sqrt{s} = 5.5$ TeV. T_f is in GeV, $B^{1/4}$ in MeV, and r_f is in fm. Solid, dotted, and dashed curves correspond to $A = 200$, 100, and 50 respectively. These plots correspond to $\Delta z_i = 1$ fm in Eq.(4).

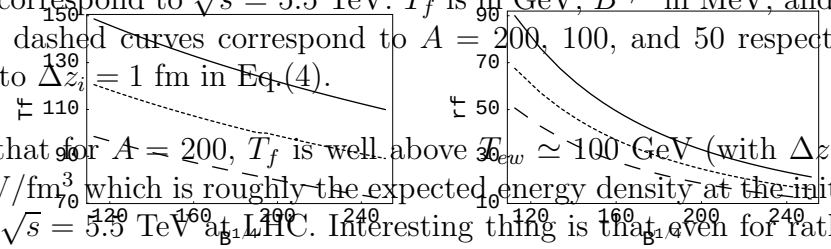

We see that for $A = 200$, T_f is well above $T_{ew} \simeq 100$ GeV (with $\Delta z_i = 1$ fm) even for $\epsilon_i \simeq 1.3$ TeV/fm^3 which is roughly the expected energy density at the initial stage in Pb-Pb collision at $\sqrt{s} = 5.5$ TeV at LHC. Interesting thing is that even for rather small values of $A = 50$, it is possible to get $T_f > T_{ew}$ by using large values of $\sqrt{s}$. This is important since early freezeout is more natural for small values of A. Note that even for the largest value of ϵ_i considered here (about 5 TeV/fm^3), the expected temperature of the QGP at the initial stage is only of the order of 1 GeV.

Fig.5 shows similar plots for the case when Δz_i in Eq.(4) is equal to 0.15 fm. Resulting temperatures are much smaller now, and for $\sqrt{s} = 5.5$ TeV resulting T_f is smaller than $T_{ew} \sim 100$ GeV. However, given the uncertainties in various parameters of the model one should still allow the possibility that T_f may exceed T_{ew} even in this case. For higher values of $\sqrt{s}$, T_f exceeds T_{ew} which should provide strong motivation for going for large values of $\sqrt{s}$ at LHC.

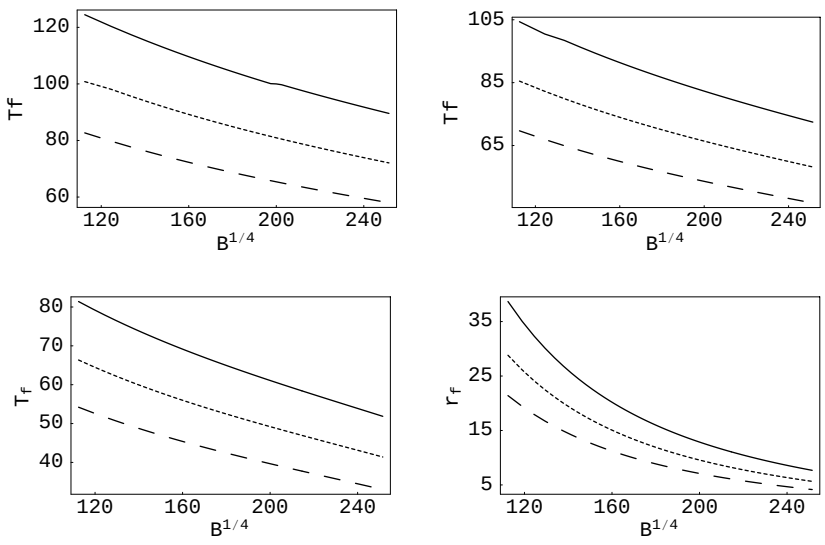

FIG. 5.
Plots with $\Delta z_i = 0.15$ fm (Eq.(4)). Figures on top left and top right correspond to $\sqrt{s} = 30$ and 15 TeV, respectively. Bottom two figures correspond to $\sqrt{s} = 5.5$ TeV. T_f is in GeV, $B^{1/4}$ in MeV, and r_f is in fm. Solid, dotted, and dashed curves correspond to $A = 200$, 100, and 50 respectively.

For RHIC, with $\sqrt{s} = 130$ GeV, for Au-Au collision, we find that T_f remains below about 30 GeV. In fact, for $\Delta z_i = 0.22$ fm, T_f is very low, and even for $A = 200$ remains below about 3.5 GeV. (Note that $T_f = 3.5$ GeV is obtained at the stage during the expansion of the hot spot, when its size is about $(3.5 \text{ GeV})^{-1}$.) Fig.6 shows plots of T_f and the corresponding values of shell radii, both for $\Delta z_i = 1$ fm, and 0.22 fm. For plots with $\Delta z_i = 0.22$ fm, no solution for T_f is found for large values of $B^{1/4}$. Thus, the range of values of $B^{1/4}$ is chosen appropriately for these plots. It is clear from these plots that the possibility of baryon violation seems out of range at RHIC. However, the possibility that temperature of the hot spot may reach a value near 30 GeV, should imply strong signatures in terms of large P_T partons, enhanced thermal production of heavy quarks, and even the possibility of Higgs and top quark production, as the net energy of the hot spot may be as high as 1 TeV. As Fig.6 shows, T_f decreases rapidly with A. Also, the situation regarding the initial energy density, and the size of the total plasma region (in the deconfined phase) is not as clear for the hadron-hadron case. For these reasons, we do not discuss the case of hadron-hadron collisions in this paper. However, for large values of $\sqrt{s}$, a hot spot with significantly large value of T_f may arise even for this case. Certainly, as we argued earlier, a shell picture

with deconfined interior seems more natural for small values of A, so should work better for hadron-hadron collisions.

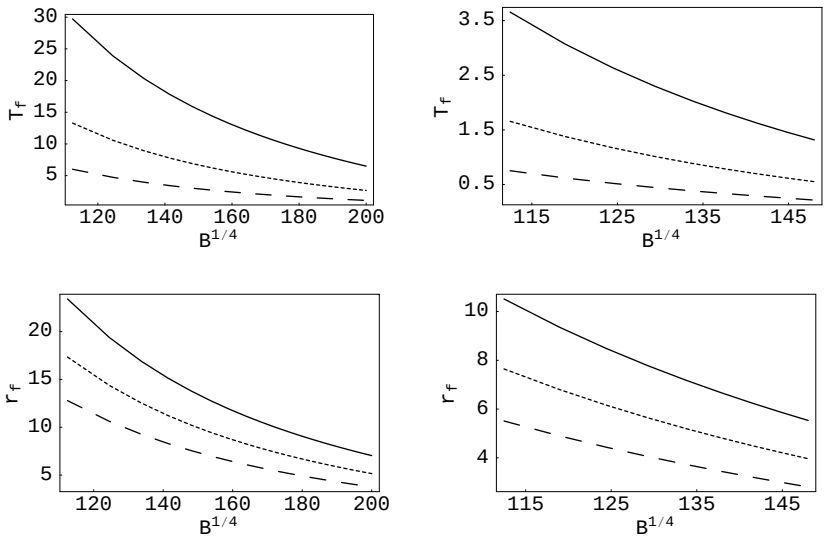

FIG. 6.
Plots for $\sqrt{s} = 130$ GeV. Figures on top left and top right correspond to Δz_i (Eq.(4)) = 1 fm and 0.22 fm respectively. Figures below these give corresponding plots of the shell radius r_f. Solid, dotted, and dashed curves correspond to $A = 200$, 100, and 50 respectively.

We have repeated the entire analysis for the case when entropy is conserved during parton expansion. In this case values of T_f are much smaller. We quote some values here to give an idea of the typical range of values of T_f for this case for various parameter values. For $A = 200$, $\sqrt{s} = 30$ TeV, and with $\Delta z_i = 1$ fm, we get T_f varying from 110 GeV to about 95 GeV as $B^{1/4}$ increases from 120 MeV to 240 MeV. For $\sqrt{s} = 15$ TeV, the corresponding values of T_f range from 95 GeV to about 80 GeV. For $\sqrt{s} = 5.5$ TeV, T_f ranges from 80 GeV to 65 GeV for the same range of $B^{1/4}$. For $\Delta z_i = 0.15$ fm, T_f ranges from 55 GeV to 40 GeV for $\sqrt{s} = 30$ TeV. We mention again, as discussed above, due to non-equilibrium conditions, energy conserving expansion may be more appropriate in our case.

VI. DISCUSSION AND CONCLUSIONS

The possibility of getting $T_f > T_{ew}$ will have startling implications. Most important of them being the possibility of unsuppressed baryon number violation via sphaleron processes

[5–7]. An important issue in this regard is the size of the region. Below T_{ew}, when electroweak symmetry is broken, sphaleron is a solution of classical equations of motion. Baryon number violating processes are dominated by sphalerons with a size of order $(3\text{ GeV})^{-1}$ [6]. This is a very large region compared to the size we have considered above, i.e. $(100\text{ GeV})^{-1}$. If we consider the size of the hot spot to be about $(3GeV)^{-1}$, then resulting values of T_f (from Eqs.(7)-(10)) never exceed about 15 GeV.

It is not clear what really should be the lower limit for the size of the region for sphaleron interactions to occur at $T > T_{ew}$ (i.e. in the symmetric phase) [6,7]. It is possible that in the symmetric phase, sphaleron processes in smaller regions may not be too suppressed [6]. Even in the symmetry broken phase, the core of sphaleron is only about $(20\text{ GeV})^{-1}$ large [7]. For hot spot of size $\sim (20\text{ GeV})^{-1}$, we find that T_f is less than about 65 GeV, even with $A = 200$, and $\sqrt{s} = 30$ TeV (with $\Delta z_i = 1$ fm).

It will certainly be remarkable if baryon violation could be observed in relativistic heavy-ion collisions. At this stage of uncertainties of this model, it is not possible to estimate how much baryon violation can be expected in a given event. (For example, small size of the hot spot may lead to extra suppression for the sphaleron rates.) One will need such estimate to come up with experimentally viable signals. If one could count each single baryon and antibaryon, then it will be straightforward to detect baryon violation. With present design of detectors, it may be more practical to measure the fluctuations in baryon number in different rapidity bins in the presence of baryon violating processes. The possibility of hot spot discussed here with temperatures very large compared to the maximum expected temperature of the initial plasma (as given by the initial energy density ϵ_i) will have many other obvious signals. For example, one will expect increased production of heavy quarks (e.g. top quark). There should be anomalous production of very large P_T partons, dileptons, and photons (depending on what is the distribution of the decay product from the decay of colliding bubble walls). From plots in Fig.6 it is clear that the possibility of baryon number violation is excluded for RHIC energies. However, if a shell like structure arises at such energies, so that one still gets a hot spot with high value of T, then some of the other signals of the hot spot, as discussed above, may still be observable. This is important because even in a situation when the bubble collapse does not proceed to sizes much smaller than 1 fm (for example if the center of the shell is not entirely devoid of partons, or if the bubble breaks up due to asphericity before collapsing to very small sizes), the resulting temperature for this 1 fm size hot spot may not be very large, but could still be larger than the initial temperature of the plasma, as determined by ϵ_i in Eq.(1). These other signals should still be relevant for detecting such a hot spot.

In conclusion, we have discussed the possibility that under certain situations, when a shell like expanding parton system emerges from the collision of ultra-relativistic nuclei, a bubble of pure false vacuum may be left behind. This shell structure of the parton system is the only non-trivial assumption in our model (that too is supported by various investigations [8]). We find that the net energy of this bubble may be a significant fraction of the total energy of the initial parton system. This bubble undergoes free, relativistic collapse. Due to extremely large Lorentz contraction factor, the bubble wall thickness decreases faster than the bubble radius. Due to this, bubble contraction proceeds down to very small scales, much smaller than the typical QCD scale of 1 fm. Eventually bubble walls collide, converting all of their kinetic energy (which equals the initial bubble energy) into particles. These

particles may eventually thermalize, leading to a hot spot. We have estimated the expected temperatures in this hot spot and find that it may be possible to get $T > T_{ew} \simeq 100$ GeV in a region of size about $(100 \text{ GeV})^{-1}$. This will restore electroweak symmetry in this tiny region, suggesting the remarkable possibility of observing baryon number violation due to unsuppressed sphaleron processes in heavy-ion collisions. There will be other signals of such hot spots, such as increased production of heavy quarks, very large P_T partons, dileptons, photons etc.

ACKNOWLEDGEMENTS

We are very thankful to Pankaj Agrawal, Sanatan Digal, Avijit Ganguly, Amit Kundu, Biswanath Layek, Shashi Phatak, and Supratim Sengupta for useful discussions and comments.

REFERENCES

[1] U. Heinz, Nucl. Phys. **A685**, 414 (2001) ; N.V.Eijndhoven, hep-ph/0012149.

[2] B.B. Back et al. (The PHOBOS Collaboration), Phys. Rev. Lett. **85**, 3100 (2000).

[3] M.A. Stephanov, Nucl. Phys. **A661**, 403 (1999); M. Stephanov, K. Rajagopal, and E. Shuryak, Phys. Rev. Lett. **81**, 4816 (1998); M. Alford, K. Rajagopal, and F. Wilczek, Phys. Lett. **B422**, 247 (1998).

[4] A. Ringwald, Nucl. Phys. **B330**, 1 (1990); L. McLerran, A. Vainshtein, and M. Voloshin, Phys. Rev. **D42**, 171 (1990); V.V. Khoze and A. Ringwald, Nucl. Phys. **B355**, 351 (1991); D.I. Diakonov and V. Yu Petrov, Phys. Lett. **B275**, 459 (1992); M.J. Gibbs, A. Ringwald, B.R. Webber, and J.T. Zadrozny, Z. Phys. **C66**, 285 (1995); See also, V.A. Rubakov and M.E. Shaposhnikov, Phys. Usp. **39**, 461 (1996), and references therein.

[5] For reviews see, A.G. Cohen, D.B. Kaplan and A.E. Nelson, Annu. Rev. Nucl. Part. Sci. **43** (1993) 27; M. Trodden, Rev. Mod. Phys. **71** (1999) 1463.

[6] P. Arnold and L. McLerran, Phys. Rev. **D36**, 581 (1987); O. Philipsen, Phys. lett. **B358**, 210 (1995).

[7] F.R. Klinkhamer and N.S. Manton, Phys. Rev. **D30**, 2212 (1984).

[8] C. Greiner and D.H. Rischke, Phys. Rev. **C54**, 1360 (1996); A. Abada and J. Aichelin, Phys. Rev. Lett. **74**, 3130 (1995);

[9] D. Teaney and E.V. Shuryak, Phys. Rev. Lett. **83**, 4951 (1999).

[10] J.D. Bjorken, K.L. Kowalski and C.C. Taylor, in *Results and Perspectives in Particle Physics 1993*; Proceedings of the 7th Rencontres de Physique de la Vallee d'Aoste, La Thuile, Italy, 1993, edited by M. Greco (Editions Frontieres, Gif-sur-Yvette, France, 1993); G. Amelino-Camelia, J.D. Bjorken, and S.E. Larsson, Phys. Rev. **D56**, 6942 (1997);

[11] I.N. Mishustin and O. Scavenius, Phys. Rev. Lett. **83**, 3134 (1999).

[12] S.A. Bass and A. Dumitru, Phys. Rev. **C61**, 064909 (2000); A. Dumitru, Phys. Lett. **B463**, 138 (1999).

[13] T. Csorgo and L.P. Csernai, Phys. Lett. **B333**, 494 (1994); J.P. Bondorf, H. Feldmeier, I.N. Mishustin, and G. Neergaard, nucl-th/0012029.

[14] K.J. Eskola, K. Kajantie, P.V. Ruuskanen, and K. Tuominen, Nucl. Phys. **B570**, 379 (2000).

[15] K.J. Eskola, P.V. Ruuskanen, S.S. Rasanen, and K. Tuominen, hep-ph/0104010.

[16] A. Krasnitz and R. Venugopalan, Phys. Rev. Lett. **84**, 4309 (2000); N. Hammon, H. Stocker, and W. Greiner, Phys. Rev. **C61**, 014901 (1999).

[17] J.D. Bjorken, Phys. Rev. **D27**, 140 (1983).

[18] L.P. Csernai and I.N. Mishustin, Phys. Rev. Lett. **74**, 5005 (1995).

[19] L. Kofman, A. Linde, and A.A. Starobinsky, Phys. Rev. Lett. **76**, 1011 (1996); S. Khlebnikov, L. Kofman, A. Linde, and I. Tkachev, Phys. Rev. Lett. **81**, 2012 (1998); I.Tkachev, S. Khlebnikov, L. Kofman, and A. Linde, Phys. Lett. **B440**, 262 (1998); M.F. Parry and A.T. Sornborger, Phys. Rev. **D60**, 103504 (1999).

[20] S. Digal and A.M. Srivastava, Phys. Rev. Lett. **80**, 1841 (1998).

[21] L.D. McLerran and B. Svetitsky, Phys. Rev. **D24**, 1981 (1981); B. Svetitsky, Phys. Rept. **132**, 1 (1986).

[22] For reviews, see, A. Albrecht, astro-ph/0007247; K.A. Olive, Phys. Rept. **190**, 307 (1990).
[23] N. Borghini, W.N. Cottingham, and R. V. Mau, J.Phys. **G26**, 771 (2000).
[24] S.C. Phatak, Phys. Rev. **C58**, 2383 (1998).
[25] H.B. Nielsen and A. Patkos, Nucl. Phys. **B195**, 137 (1982); L.R. Dodd, A.G. Williams, and A.W. Thomas, Phys. Rev. **D35**, 1040 (1987); A. Drago, M. Fiolhais, and U. Tambini, Nucl. Phys. **A588**, 801 (1995); A. Mazzolo, J.-F. Mathiot, and R.M. Galain, Phys. Lett. **B274**, 154 (1992).
[26] J. Ignatius, K. Kajantie, H. Kurki-Suonio, and M. Laine, Phys. Rev. **D49**, 3854 (1994).
[27] L.P. Csernai and J.I. Kapusta, Phys. Rev. **D46**, 1379 (1992).
[28] J.C. Miller and O. Pantano, Phys. Rev. D **40**, 1789 (1989); **42**, 3334 (1990).
[29] M.B. Voloshin, I.Yu. Kobzarev and L.B. Okun, Yad. Fiz. **20**, 1229 (1974) [Sov. J. Nucl. Phys. **20**, 644 (1975)]; S. Coleman, Phys. Rev. **D15**, 2929 (1977).
[30] A.M. Srivastava, Phys. Rev. **D45**, R3304 (1992).
[31] E. Witten, Phys. Rev. D **30**, 272 (1984); S.A. Bonometto and O. Pantano, Phys. Rep. **228**, 175 (1993).
[32] P. Danielewicz and M. Gyulassy, Phys. Rev. **D31**, 53 (1985).
[33] R. Venugopalan, Nucl. Phys. **A590**, 147c (1995).
[34] L. Susskind, Phys. Rev. **D49**, 6606 (1994).
[35] L.M. Widrow, Phys. Rev. **D40**, 1002 (1989).
[36] D.W. Neilsen and M.W. Choptuik, Class. Quant. Grav. **17**, 733 (2000).